JOURNAL OF APPLIED ELECTROCHEMISTRY 8 (1978) 515–522

Application of DSA-type electrodes to a positive grid in lead-acid batteries

M. INAI, C. IWAKURA, H. TAMURA

Department of Applied Chemistry, Faculty of Engineering, Osaka University, Suita, Osaka, Japan

Received 3 January 1978

The possibility of the use of modified DSA-type electrodes as positive grids in lead–acid batteries was examined by anodic polarization measurements, charge–discharge tests and self-discharge tests of the Ti/RuO_2 and $Ti/RuO_2/\beta$-PbO_2 electrodes. The passivation of a titanium base was retarded by using a very thin film of ruthenium dioxide. The $Ti/RuO_2/\beta$-PbO_2 electrode could be used as a positive grid to a certain extent. On the other hand, the Ti/RuO_2 electrode showed the worse characteristics for the positive grid, mainly due to the low oxygen overvoltage of the ruthenium dioxide layer. Some other problems to be solved have also been pointed out.

1. Introduction

The desired features of grid materials in lead–acid batteries are conductivity, strength, corrosion resistance, passivation resistance, electrochemical 'cleanliness', compatibility with active material (adherence), fabricability (casting or working, joining) and lightweight, according to Perkins *et al.* [1]. Of these, corrosion resistance of the positive grid is of particular importance because the corrosion produces many undesirable effects during the battery operation and often determines the battery service life. Strength is also very important for high power and high energy density batteries. Considerable savings in battery weight as well as volume could be achieved by using a grid such as titanium.

Titanium has very useful properties which would be exploited in batteries; an excellent resistance to corrosion, a high mechanical strength and a light weight. Therefore, titanium has been suggested by Cotton and Dugdale [2] as a substitute for lead or lead alloys as a grid material. Since titanium tends to form a passivating oxide film over its surface, a suitable conductive coating must be applied to the titanium surface in order to maintain the conductive function of the grid. Cotton and Dugdale [2] experimentally accomplished this by first electroplating platinum on the passive film and following this by a layer of lead dioxide. Some work of the same kind has been reported in the patent literature; e.g., titanium base/PbO_2 electrodeposit [3] and titanium base/gold or lead plating/PbO_2 electrodeposit [4].

However, the use of a more favourable coating material which easily forms a solid solution with titanium dioxide at the surface of the titanium base can be expected to improve the characteristics of the titanium positive grids by acting to reduce passivation and to increase adhesion. The present authors [5] have investigated the electrochemical characteristics of DSA-type electrodes such as ruthenium dioxide covered titanium. In this work, ruthenium dioxide was employed on trial as the coating material because both TiO_2 (rutile) and RuO_2 have rutile structures with very similar cell dimensions and further because the active material, and β-PbO_2, also have the same crystal structure. However, it should be noted that the use of ruthenium dioxide may result in a low charging efficiency and a high self-discharge rate in lead–acid batteries since it has the lowest oxygen overvoltage ever observed. Such problems can be solved by the replacement of ruthenium dioxide by other oxides having the same crystal structure but a higher oxygen overvoltage. The preliminary work on this has been reported briefly in the previous paper [6]. This paper describes further details of the possible use of the ruthenium

dioxide covered titanium grid, together with the data for other related grids.

2. Experimental

The ruthenium dioxide coating was achieved by thermal decomposition of ruthenium trichloride on a smooth titanium sheet (2·54 cm^2). The details of the preparative procedure were described in the previous paper [7]. The amount of ruthenium dioxide loadings were in the range 10^{-6}–10^{-8} mol cm^{-2} in this work. The resulting electrode will be referred to as a Ti/RuO_2 grid. In some experiments, a β-PbO_2 layer was electrodeposited on the Ti/RuO_2 grid from the plating bath of 21% $Pb(NO_3)_2$ at 60° C with a current density of 54 mA cm^{-2} for 3 min. The presence of a thin layer of ruthenium dioxide on a titanium base facilitates the subsequent electrodeposition of β-PbO_2. The electrode will be designated as a $Ti/RuO_2/\beta$-PbO_2 grid to distinguish it from the grid described above. For comparison with these two grids, a lead sheet with the same size was also used as a positive grid.

A standard pasting procedure was employed in the preparation of the positive plates. The weight of paste was represented in the figures by the number of grams per 2.54 cm^2 of grid surface in the wet condition. After pasting, the plates were formed in 1·050 sp. gr. H_2SO_4 prior to use in the various tests. The tests include the charge–discharge test and the self-discharge test of the plates.

All electrochemical measurements except for the galvanostatic charge–discharge test were carried out in 1·290 sp. gr. H_2SO_4 at 25° C. A platinum sheet counter-electrode and a mercury–mercurous sulphate (Hg/Hg_2SO_4) reference electrode were used. In the galvanostatic charge–discharge test, a spongy lead with large capacity was used as the counter-electrode and the electrolyte was 1·300 sp. gr. H_2SO_4. With the exception of the geometric area of 0·64 cm^2 for the galvanostatic charge–discharge test, the geometric area of the grids or the plates exposed to the solution was reduced to 1 cm^2 by using a Teflon holder (Fig. 1). The detailed measuring conditions will be given separately in the next section.

3. Results and discussion

3.1. *Anodic characteristics of grids*

Since a positive plate in a lead–acid battery is usually charged at constant current densities of 5–10 mA cm^{-2}, the stability of the Ti/RuO_2, $Ti/RuO_2/\beta$-PbO_2 grid and the Ti/RuO_2/paste plate were tested under the galvanostatic condition at 10 mA cm^{-2}. Fig. 2 shows the variations of potential with polarization time for the grid and the

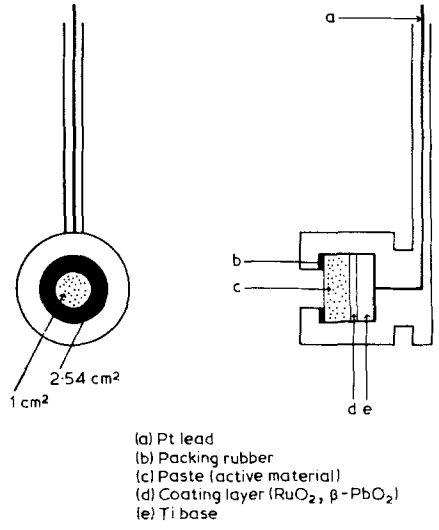

Fig. 1. Schematic drawing of the test electrode and its holder.

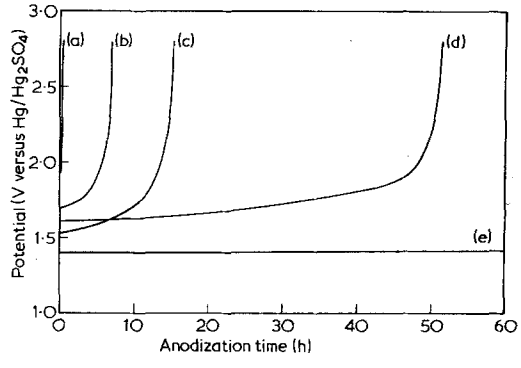

Fig. 2. Variation of potential with anodization time under galvanostatic conditions at 10 mA cm^{-2}:
(a) Ti/RuO_2 (2×10^{-8} mol cm^{-2})
(b) Ti/RuO_2 (5×10^{-8} mol cm^{-2})
(c) Ti/RuO_2 (1×10^{-7} mol cm^{-2})
(d) Ti/RuO_2 (1×10^{-7} mol cm^{-2})/β-PbO_2 (5×10^{-5} mol cm^{-2})
(e) Ti/RuO_2 (1×10^{-7} mol cm^{-2})/paste (756 mg/2·54 cm^2).

plate in 1·290 sp. gr. H_2SO_4. From these results, it was found that the durability of the grid increases with increasing the amount of RuO_2 loadings and the thin film of ruthenium dioxide is fairly effective for preventing the passivation of the titanium base. The calculated thickness of the ruthenium dioxide layer is about 20 nm when the amount of the RuO_2 loading is 10^{-7} mol cm^{-2}. It is clear that the service life of the Ti/RuO_2 grid is further improved by the electrodeposition of β-PbO_2 on its surface. Evidently, the Ti/RuO_2/paste plate was quite stable under these conditions during the whole period examined.

In order to charge the positive plate efficiently with a minimum loss of current in the possible side reaction of oxygen evolution from the surface of the Ti/RuO_2 grid, the optimum amount of RuO_2 loadings on the titanium base should be defined. So, the oxygen evolution current on the Ti/RuO_2 grid was evaluated by means of cyclic voltammetry with a sweep rate of 10 mV s^{-1} in the potential region of + 0·75–1·65 V. Fig. 3 shows the plot of oxygen evolution current at 1·65 V against the amount of RuO_2 loading. The linear relationship can be found between them and it is formulated as

$$\log i = k \log [RuO_2] + \text{const.} \qquad (1)$$

where k denotes the slope of the straight line and is very close to unity. The same relationship has been reported by Yeager *et al.* [7] in alkaline solution. For the Ti/RuO_2 grid with the amount of RuO_2 loading lower than 2×10^{-8} mol cm^{-2}, the oxygen evolution current deviated from the straight line due to the formation of a TiO_2 film

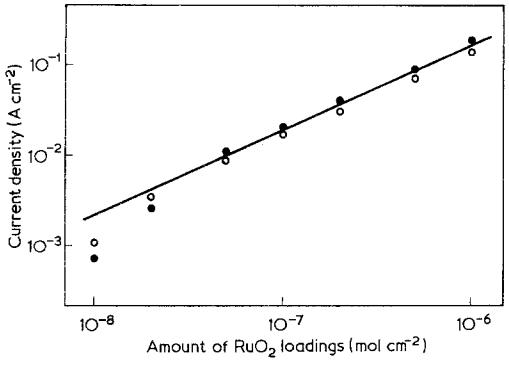

Fig. 3. Plots of oxygen evolution current at 1·65 V against amount of RuO_2 loading
○, first cycle
●, tenth cycle.

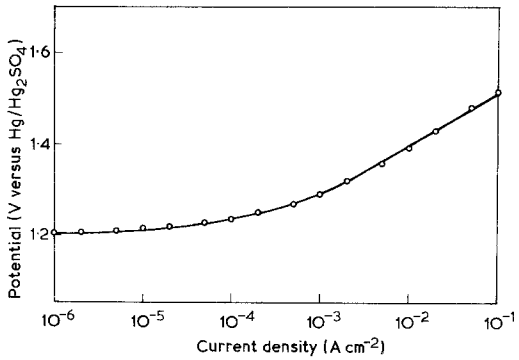

Fig. 4. Anodic polarization curve obtained galvanostatically on Ti/RuO_2/paste plate in O_2-saturated 1·290 sp. gr. H_2SO_4 at 25° C.

on the titanium base. Therefore, the amount of RuO_2 loading was kept constant (1×10^{-7} mol cm^{-2}) in most of the later experiments.

The rest potential of the Ti/RuO_2/paste plate was + 1·185 V versus Hg/Hg_2SO_4 in 1·290 sp. gr. H_2SO_4 at 25° C, while that of the pure lead electrode was − 0·955 V versus Hg/Hg_2SO_4. Accordingly, the open-circuit voltage of the cell will be about 2·14 V, which agrees with that for the usual lead–acid battery. The typical anodic polarization curve of the plate, obtained galvanostatically with decreasing current, is shown in Fig. 4. For the polarization curve, the ohmic drop was corrected by using an interruptor technique. The plate was stable against the anodic polarization, and gave an anodic Tafel line with a slope of 0·12 V in 1·290 sp. gr. H_2SO_4. This value is in fair agreement with that reported for oxygen evolution on a β-PbO_2 electrode [8], but not on RuO_2 and Ti/RuO_2 electrodes [9]. From these facts, it has become apparent that the Ti/RuO_2 grid acts as an inert but conducting support during the charging of the positive plate.

3.2. *Charge–discharge characteristics of plates*

The charge–discharge characteristics of the plates were measured under both potentiostatic and galvanostatic conditions. The potentiostatic test was carried out by means of cyclic voltammetry, in which the potential was swept between + 0·75 and + 1·65 V with a sweep rate of 0·25 mV s^{-1} (2 h cycle^{-1}). In the galvanostatic test, the charging of plates was done at 6·68 mA/0·64 cm^2 for 105 min, followed by discharging at 36 mA/

0·64 cm^2 for 15 min, and this operation was repeated many times

The cyclic voltammograms of the Ti/RuO_2/β-PbO_2/paste plate as well as the Ti/RuO_2/paste plate were similar to those of the Pb/paste plate. The discharging capacity of the plates was evaluated from the area of the cathodic peak in the voltammogram, and the variation of discharging capacity with number of cycles is shown in Fig. 5. It is evident from this figure that these two plates have approximately the same tendency of change in capacity. The capacities decreased gradually with increasing the number of cycles, and finally there was a sharp decrease, mainly due to the shedding of the paste, or the active material. The discharge efficiency of the Ti/RuO_2/β-PbO_2/paste plate was comparable to that of the Pb/paste plate in these tests.

In order to retard the shedding of the paste, a plastic sheet having micropores* was placed on the positive plate so that the sheet behaved like a glass fibre retainer mat prior to the forming of the plate. Using this type of plate, the charge–discharge tests were done under the same conditions as in the above-mentioned tests, and the results are shown in Fig. 6 as a plot of the discharging capacity against the number of cycles. Evidently, the service life of the positive plates was prolonged to a great extent. After cycling for more than about

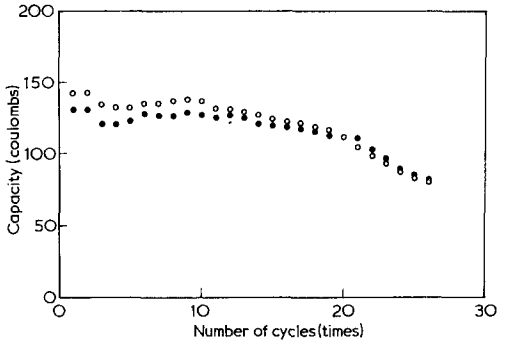

Fig. 5. Variation of discharging capacity with number of cycles in 1·290 sp. gr. H_2SO_4
○, Ti/RuO_2 (1 × 10^{-7} mol cm^{-2})/β-PbO_2 (5 × 10^{-5} mol cm^{-2})/paste (745 mg/2·54 cm^2)
●, Pb/paste (775 mg/2·54 cm^2)

* The plastic sheet 'Yumicron' was supplied from the Yuasa Battery Co. Ltd and has the following specifications: thickness, 0·1–0·2 mm; mean electrical resistance, 0·0002–0·0004 Ω dm^{-2}; mean pore diameter, 0·1–1 μm; porosity, 60%.

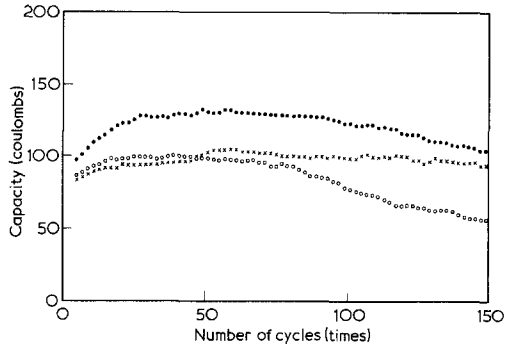

Fig. 6. Variation of discharging capacity with number of cycles in 1·290 sp. gr. H_2SO_4
○, Ti/RuO_2 (1 × 10^{-7} mol cm^{-2})/β-PbO_2 (5 × 10^{-5} mol cm^{-2})/paste (735 mg/2·54 cm^2)
●, Ti/RuO_2 (1 × 10^{-7} mol cm^{-2})/β-PbO_2 (5 × 10^{-5} mol cm^{-2})/paste (806 mg/2·54 cm^2)
×, Pb/paste (829 mg/2·54 cm^2)
All plates were covered with a plastic film having micropores. In the case of the experiment marked ●, the potential was swept between 0·70 and 1·70 V (versus Hg/Hg_2SO_4) with a sweep rate of 0·25 mV s^{-1} (8000 s $cycle^{-1}$).

80 times, the drop in discharging capacity became appreciable for the Ti/RuO_2/β-PbO_2/paste plate, compared with the Pb/paste plate. This is attributable to a decrease in the charging efficiency for the former plate under the potentiostatic conditions, probably due to oxygen evolution on the ruthenium dioxide layer and an increased ohmic resistance at the Ti/RuO_2 interface. Therefore, the discharging efficiency can be expected to be increased by widening the potential sweep range. The data obtained for the Ti/RuO_2/β-PbO_2/paste plate in the wider potential sweep range are shown in Fig. 6. The charge–discharge characteristics of the plate are clearly improved as expected.

Figs. 7 and 8 show the variations of terminal voltage with time at a given number of cycles in the galvanostatic charge–discharge test. In this case, the variation in terminal voltage is considered to correspond to that in the potential of the test plates because the capacity of the spongy lead counter-electrode was about 50 times larger than the capacity of the test electrodes. It can be seen from these two figures that under these test conditions the service lives of the Ti/RuO_2/paste, Ti/RuO_2/β-PbO_2/paste and Pb/paste plate were 35, 115 and over 140 cycles, respectively. At the end of the service lives, the drop and the rise in terminal voltage were clearly observed for dis-

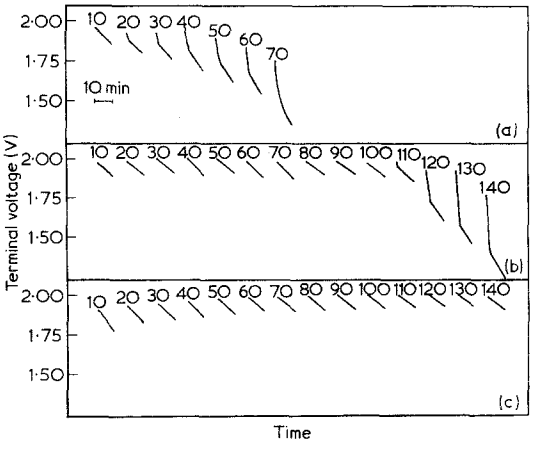

Fig. 7. Variation of terminal voltage with time at given numbers of discharges
(a) Ti/RuO_2 (1×10^{-7} mol cm^{-2})/paste (443 mg/1·43 cm^2)
(b) Ti/RuO_2 (1×10^{-7} mol cm^{-2})/β-PbO_2 (5×10^{-5} mol cm^{-2})/paste (432 mg/1·43 cm^2)
(c) Pb/paste (441 mg/1·43 cm^2).

charging and charging curves, respectively, indicating that the internal ohmic resistance of the plates was increased. The internal ohmic resistance of the plates is roughly divided into two components, i.e. paste (active material) and grid. In the present case, however, the increase in ohmic resistance of the grids was presumed to be a major cause of the increased internal ohmic resistance of the plates.

After the galvanostatic test, the morphologies of the plates were examined by scanning electron microscopy (SEM) in order to verify the above presumption. Some results obtained for the $Ti/RuO_2/\beta$-PbO_2/paste plate after 137 discharges are presented in Fig. 9. Figs. 9a and b show the front of the paste (facing the electrolyte) and the back (facing the $Ti/RuO_2/\beta$-PbO_2 grid), respectively. On both sides, the paste was mainly composed of porous PbO_2, and lead sulphate was only a minor part of the paste in spite of the end of discharge conditions prevailing. These phenomena were also observed for the Ti/RuO_2/paste plate. On the other hand, many fine crystals of $PbSO_4$ were observed in the case of the Pb/paste plate. It is therefore concluded that the increased internal ohmic resistance of the Ti/RuO_2/paste, and $Ti/RuO_2/\beta$-PbO_2/paste plate did not result from the increase in the resistance of the paste. Fig. 9c shows a microphotograph of the grid–paste interface in the $Ti/RuO_2/\beta$-PbO_2/paste plate after 137 cycles. The upper and lower sides correspond to the paste and the electrodeposited β-PbO_2 layer, respectively. The morphology of the close-packed layer with some porous PbO_2 parts was clearly observed in the β-PbO_2 layer. The porous PbO_2 parts were considered to have undergone charge and discharge, and the penetration of the electrolyte through the porous PbO_2 parts might lead to the passivation of the titanium base.

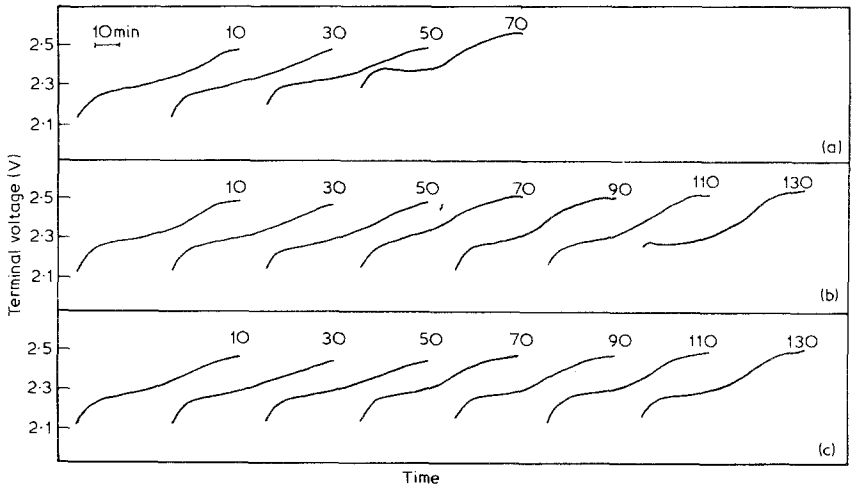

Fig. 8. Variation of terminal voltage with time at given numbers of charges
(a) Ti/RuO_2 (1×10^{-7} mol cm^{-2})/paste (443 mg/1·43 cm^2)
(b) Ti/RuO_2 (1×10^{-7} mol cm^{-2})/β-PbO_2 (5×10^{-5} mol cm^{-2})/paste (432 mg/1·43 cm^2)
(c) Pb/paste (441 mg/1·43 cm^2)

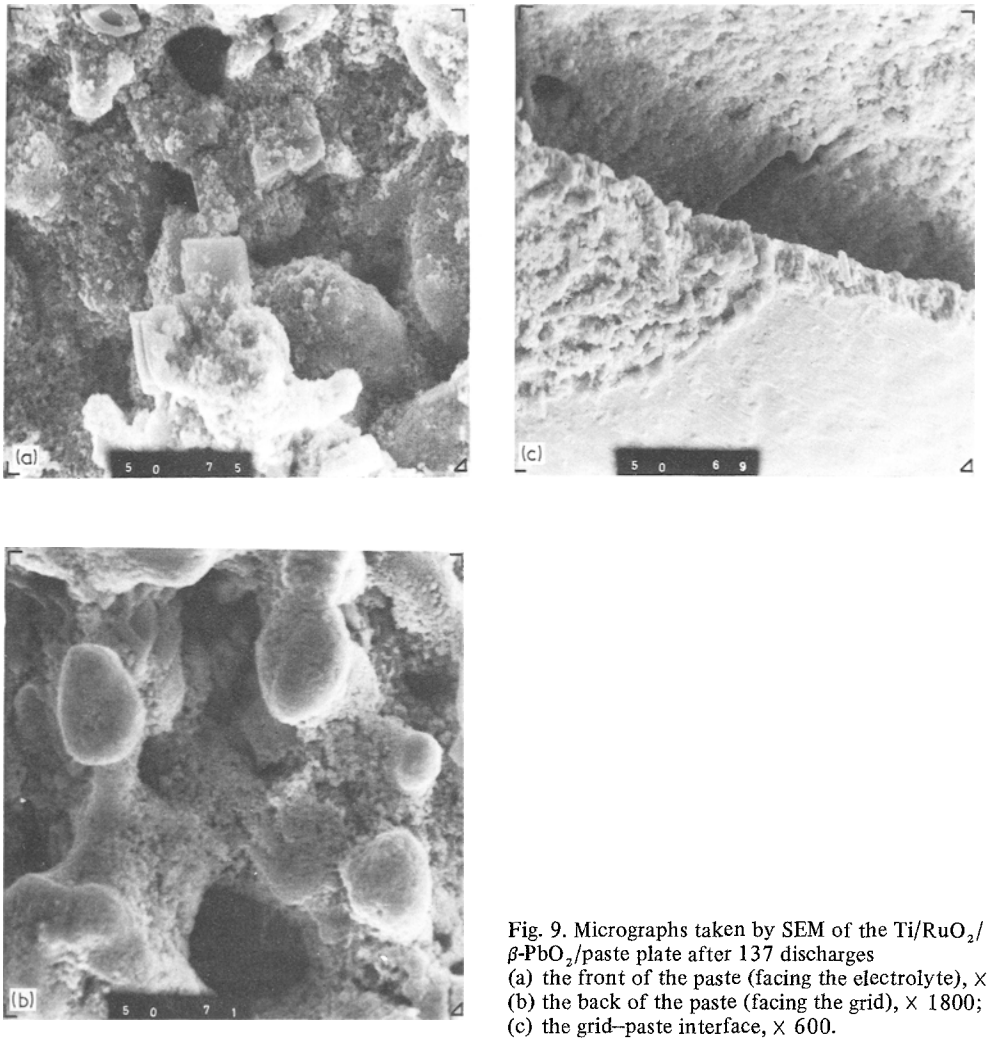

Fig. 9. Micrographs taken by SEM of the Ti/RuO_2/β-PbO_2/paste plate after 137 discharges
(a) the front of the paste (facing the electrolyte), × 1800;
(b) the back of the paste (facing the grid), × 1800;
(c) the grid–paste interface, × 600.

3.3. *Self-discharging characteristics of the plates*

The self-discharge characteristics of the plates were examined by the measurement of capacity loss after standing for 16 days. In this measurement, the plates were charged at 3·8 mA cm^{-2} for 19 h, and the discharging current (16 mA cm^{-2}) was cut when the potential reached + 0.70 V versus Hg/Hg_2SO_4 at the end of discharge. The surface of the plates was covered with the plastic sheet in order to diminish the capacity loss resulting from the shedding of the paste, in the same manner as described previously. The self-discharge rate was then calculated by using the following equation.

$$\text{Self-discharge rate (\%/day)} = \left(1 - \frac{2C_2}{C_1 + C_3}\right)\frac{100}{D} \quad (2)$$

where C_1 is a mean value of the discharging capacities measured four times before standing, C_2 the discharge capacity measured immediately after standing, and C_3 the discharging capacity measured immediately after the measurement of C_2, followed by complete charging. D denotes the number of days for standing.

The self-discharge rates obtained in this way are summarized in Table 1. As can be seen from this table, the self-discharge rate increased in the order

Table 1. Self-discharge rates of the three plates

Plate	*Self-discharge rate* (% day^{-1})
Ti/RuO_2(1×10^{-7} mol cm^{-2})/paste (743 mg/2·54 cm^2)	5·4
Ti/RuO_2(1×10^{-7} mol cm^{-2})/β-PbO_2(5×10^{-5} mol cm^{-2})/paste (749 mg/2·54 cm^2)	0·2
Pb/paste (727 mg/2·54 cm^2)	0·3

$Ti/RuO_2/\beta$-PbO_2/paste plate < Pb/paste plate ≪ Ti/RuO_2/paste plate. It is considered that, in the case of the $Ti/RuO_2/\beta$-PbO_2/paste plate, a sulphuric acid solution was prevented from penetrating to the surface of the titanium base by the presence of a thin film of electrodeposited β-PbO_2. On the other hand, the high self-discharge rate of the Ti/RuO_2/paste plate can be explained on the basis of the local cell mechanism. The anodic reaction is oxygen evolution from water.

$$2H_2O \rightarrow O_2 + 4H^+ + 4e^- \qquad (3)$$

and the cathodic reaction is formation of lead sulphate from lead dioxide.

$$PbO_2 + H_2SO_4 + 2H^+ + 2e^- \rightarrow PbSO_4 + 2H_2O. \qquad (4)$$

In order to prove the above mechanism, the anodic polarization curves of the Ti/RuO_2 and $Ti/RuO_2/\beta$-PbO_2 grids and the cathodic polarization curves of the Pb/paste plate were measured under galvanostatic conditions. The polarization data shown in Fig. 10 are those obtained after waiting for 2 min at each point of measurement. Evidently, the oxygen overvoltage of the Ti/RuO_2 grid is very low, and hence the self-discharge rate becomes high. From the current at an intersecting point of the anodic polarization curves of the grids with the cathodic polarization curve of the Pb/paste plate, the relative self-discharge rate can be evaluated, though the true rate is very different from the relative one because of the decrease in effective surface area of the grids caused by the presence of paste. Thus, the relative self-discharge rates expressed by current are $4·0 \times 10^{-4}$ and $1·5 \times 10^{-5}$ A cm^{-2} for the Ti/RuO_2 and $Ti/RuO_2/\beta$-PbO_2 grids, respectively. The ratio of these two currents exactly agreed with the data given in Table 1.

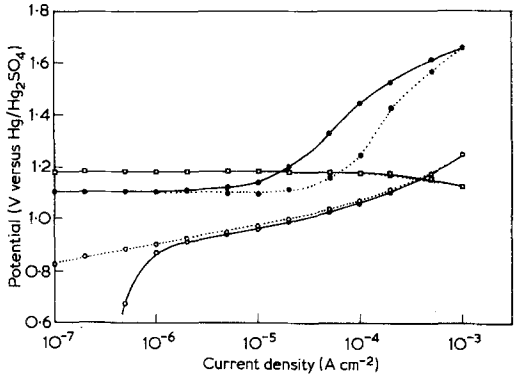

Fig. 10. Galvanostatic polarization curves in 1·290 sp. gr. H_2SO_4
○, Ti/RuO_2 (1×10^{-7} mol cm^{-2})
●, Ti/RuO_2 (1×10^{-7} mol cm^{-2})/β-PbO_2 (5×10^{-5} mol cm^{-2})
□, Pb/paste (747 mg/2·54 cm^2).
The solid and dotted lines indicate the data obtained with increasing and decreasing currents, respectively.

4. Conclusions

From the above-mentioned results, it is concluded that the passivation of a titanium base can be retarded by introducing the thin intermediate layer of ruthenium dioxide and that the $Ti/RuO_2/\beta$-PbO_2 electrode can be used to some extent as a positive grid in lead–acid batteries. With use over long times, however, the Ti/RuO_2 and $Ti/RuO_2/\beta$-PbO_2 grids being developed in this work may have the following problems: (a) The shedding of paste (active material) occurs because of the lack of the adhesion of paste to the grid, (b) the lowering of the discharging efficiency and the significant self-discharge of the plate occur because of the low oxygen overvoltage of the ruthenium dioxide layer and (c) the deterioration of the charge–discharge performance occurs because of the development of an additional ohmic resistance at the Ti/RuO_2 interface, i.e. the passivation of the titanium base. However, these problems are expected to be solved by the following modifications: (i) The ruthenium dioxide layer is replaced by other oxides having the same crystal structure (rutile-type) but higher oxygen overvoltage for solving problem (b). (ii) A sand-blasted

titanium base is used in place of the smooth titanium sheet in order to produce a good adhesion of the oxide layer to the base [problem (a)] and the least electrical interface resistance [problem (c)]. Further work is now in progress.

Acknowledgements

The authors are pleased to acknowledge the financial support of this work by the International Lead Zinc Research Organization, Inc. (New York). The authors also express their appreciation to Mr S. Hattori, Mr M. Kono and Mr J. Yamashita of the Yuasa Battery Co. Ltd for providing necessary facilities.

References

[1] J. Perkins, J. L. Pokorny and M. T. Coyle, NPS-69PS76101.

[2] J. B. Cotton and I. Dugdale, 'Batteries, Research and Development in Non-Mechanical Electric Power Sources', Proceedings of the 3rd International Symposium, (ed. D. H. Collins), Pergamon Press, New York (1963) p. 297.

[3] Electricity Council, British Patent no. 1 373 611 (November 1974).

[4] S. Ruben, US Patent no. 3 798 070 (May 1972).

[5] H. Tamura and C. Iwakura, *Denki Kagaku* **43** (1975) 674.

[6] C. Iwakura, M. Inai and H. Tamura, *Chem. Lett.* (1977) 1407.

[7] W. O'Grady, C. Iwakura, J. Huang and E. Yeager, 'Proceedings of the Symposium on Electrocatalysis', (ed. M. W. Breiter) The Electro chemical Society, Princeton (1974) p. 286.

[8] P. Rüetsch and B. D. Cahan, *J. Electrochem. Soc.* **105** (1958) 369.

[9] C. Iwakura, K. Hirao and H. Tamura, *Electrochim. Acta* **22** (1977) 335.